

# Spectrum Binning Approach for Multi-Material Beam Hardening Correction (MMBHC) in CT

Qiao Yang, Meng Wu, Nicole Maass, Andreas K. Maier, Joachim Hornegger, and Rebecca Fahrig

**Abstract**—In CT, the nonlinear attenuation characteristics of polychromatic X-rays cause beam hardening artifacts in the reconstructed images. When datasets contain multiple materials in the field of scan, the performance of state-of-the-art beam hardening correction approaches is limited by high computational load and reduced correction efficiency. An image based multi-material beam hardening correction (MMBHC) method is introduced by conserving original reconstruction attenuation in a material density map, and obtaining beam hardening artifacts by polychromatic forward projecting of the original CT images. By decomposing the attenuation coefficient into photoelectric and Compton scattering components, the spectrum can be parameterized and presented with several energy bins. In this paper, the MMBHC algorithm is accelerated by using a proposed spectrum binning (SB) method to reduce the required prior knowledge from full spectrum to three energy bins. The approach has a significant computational time reduction by use of material number independent forward projection and parameterized energy spectrum with fewer bins. Moreover, representing the spectrum with a few parameters instead of optimizing full spectrum increase the stability of the MMBHC process. The algorithm has been evaluated with a simulated phantom on 3D cone beam geometry. In comparison to correction results with full spectrum information, the results with optimized three bins spectrum shows comparable artifact reduction efficiency while providing significant reduction on computational time.

**Index Terms**—Polychromatic X-ray, beam hardening correction, spectrum binning, CT reconstruction

## I. INTRODUCTION

### A. Purpose of this work

In computed tomography (CT), analytical reconstruction techniques such as filtered backprojection (FBP) are based on the assumption that X-ray radiation is monoenergetic, and the total attenuation of incident X-rays is linearly related to the thickness of the object along the ray. In reality, X-ray beams consist of a continuous energy spectrum, and material attenuation coefficients are energy dependent. When a polychromatic X-ray passes through the substances, due to the non-linearity, reconstruction images will contain cupping and streaking artifacts, which are so-called beam hardening artifacts.

Various beam hardening correction (BHC) algorithms have been developed for X-ray CT, both analytically [1]–[3] and iteratively [4]–[7]. However, when multiple materials appear in a scanned dataset, such as contrast agent or metal implants in clinical CT or most industrial CT cases, state-of-the-art

approaches have large computational complexity and limited correction performance.

### B. State of the art

In previous work [8], a practical multi-material BHC approach which employs a CT-value conserving material decomposition technique was presented. The method separates reconstructed images into density images and images containing material information, which has the advantage that segmentation errors, which result in invalid material properties for a voxel, have only minor effects on the beam hardening correction.

It has been presented that energy dependent attenuation coefficients can be decomposed into a linear combination of photoelectric and Compton scattering components [5]. Wu et al. have proposed a modified optimization problem for polychromatic statistical reconstruction algorithms, and simplified the algorithms with a spectrum binning method to reduce the full spectrum [9]. An evaluation study to examine the robustness of the method with mismatched spectra are published in [10].

### C. Outline

In this paper, a method that applies spectrum binning to accelerate the MMBHC approach is presented. The original CT value conserving density map is combined with photoelectric and Compton scattering components which are calculated from attenuation decomposition. By polychromatic forward projecting the two components separately, polychromaticity enhanced images are obtained to calculate the beam hardening artifacts. In the next section, a review of the MMBHC approach and the spectrum binning method is given and the derivation of the combined algorithm is discussed in detail. In Section III, the results from the simulated phantom are illustrated and quantitative evaluation is performed.

## II. METHOD

### A. Multi-material beam hardening correction (MMBHC)

When a monochromatic X-ray beam traverses a homogeneous object, according to Lambert-Beer's law, the total attenuation is linearly related to the intersection length of the object and the ray. However, in practical setups, the emitted X-ray photons have varying energies and the detector response is also energy-dependent. The measured intensity of a polychromatic beam  $Y_{\text{poly}}$  on detector pixel  $i$  can be written as the sum of monochromatic contributions for each energy

Q. Yang, A. K. Maier, and J. Hornegger are with the Pattern Recognition Lab, Department of Computer Science, Friedrich-Alexander-University Erlangen-Nuremberg, Germany. E-mail: qiao.yang@cs.fau.de. M. Wu and R. Fahrig are with the Department of Radiology, Stanford University, USA. N. Maass is with the Siemens AG, Healthcare Sector, Erlangen, Germany

bin  $E$  in the X-ray spectrum ( $E \in [0, E_{max}]$ ):

$$Y_{poly,i} = \int_0^{E_{max}} b_{0,i}(E) \cdot \exp\left(-\int_{L_i} \mu(E, \mathbf{r}) dl\right) dE, \quad (1)$$

where  $b_{0,i}(E)$  is the normalized source-detector energy spectrum,  $L$  is the path length of the corresponding ray direction. Denote  $\mathbf{r}$  as the spatial location on the reconstruction grid, and  $\mu(E, \mathbf{r})$  is the spatial distribution of the attenuation coefficient which depends on spectrum energy  $E$ .

When a dataset consists of  $M$  materials, the mass attenuation coefficient for material  $m$  at specific energy  $E_0$  can be written as  $\kappa_m(E_0) = \mu_m(E_0)/\rho_m$ , with  $\rho_m$  being the reference material density. In [8], a multi-material beam hardening correction scheme is proposed, which separates reconstructed images  $g(\mathbf{r})$  into images containing material information  $\kappa_m(E)$  and spatial density images  $\rho_m(\mathbf{r})$ . Thus, (1) can be rewritten as

$$Y_{poly,i} = \int_0^{E_{max}} b_{0,i}(E) \cdot \exp\left(-\sum_{m=1}^M \kappa_m(E) \int_{L_i} \rho_m(\mathbf{r}) dl\right) dE. \quad (2)$$

Instead of using the reference material density  $\rho_m$ , material density at spatial location  $\mathbf{r}$  is applied:

$$\rho_m(\mathbf{r}) = \frac{f_m(\mathbf{r}) \cdot g_{initial}(\mathbf{r})}{\kappa_m(E_0)}, \quad (3)$$

where  $f_m(\mathbf{r})$  is the binary mask of material  $m$  that is obtained from automatic k-means segmentation [11] at location  $\mathbf{r}$ . By polychromatically forward projecting the original beam hardening affected volume  $g_{initial}$ , additional beam hardening is introduced and added up onto the existing artifacts. The difference between  $g_{initial}$  and the reconstruction image  $g_{calc}(\mathbf{r})$  from recalculated polychromatic attenuation can be used to estimate the beam hardening error:

$$\hat{g}_{BH}(\mathbf{r}) = g_{calc}(\mathbf{r}) - \text{Gauss}(0, \sigma) * g_{initial}(\mathbf{r}), \quad (4)$$

with  $\arg \min_{\sigma} \|\hat{g}_{BH}(\mathbf{r})\|_2$ . Note that a spatial resolution matching Gaussian filtering is applied. Then the beam hardening image  $\hat{g}_{BH}(\mathbf{r})$  is subtracted from the initial reconstruction to obtain a beam hardening corrected image

$$g_{corrected}(\mathbf{r}) = g_{initial}(\mathbf{r}) - \hat{g}_{BH}(\mathbf{r}). \quad (5)$$

Since errors may occur during segmentation due to severe artifacts, an iterative scheme can be used for more accurate image updates.

## B. Spectrum binning (SB)

De-Man et al. had decomposed the energy dependent attenuation coefficients into linear combinations of photoelectric and Compton scattering components [5]. Therefore, the attenuation coefficients of a certain substance can be represented as:

$$\mu_m(E) = \phi_m \Phi(E) + \theta_m \Theta(E), \quad (6)$$

where  $\Phi(E)$  and  $\Theta(E)$  are base functions of energy dependent photoelectric and Compton scattering components, and  $\phi_m$  and  $\theta_m$  represent the  $m$ th material dependence of the two

components. For a multi-material case, from (6) the attenuation coefficient can be decomposed to:

$$\begin{aligned} \mu(E, \mathbf{r}) &= \left( \Phi(E) \sum_{m=1}^M \phi_m f_m(\mathbf{r}) + \Theta(E) \sum_{m=1}^M \theta_m f_m(\mathbf{r}) \right) \\ &= \Phi(E) \phi(\mathbf{r}) + \Theta(E) \theta(\mathbf{r}). \end{aligned} \quad (7)$$

$\phi(\mathbf{r})$  and  $\theta(\mathbf{r})$  are the amount of photoelectric and scattering components from all materials at spatial location  $\mathbf{r}$ .

Using this expression, the detector signal from full spectrum information is

$$\begin{aligned} \hat{Y}^{\text{full}} &= \int_0^{E_{max}} b_0(E) \\ &\cdot \exp\left(-\Phi(E) \int_{L_i} \phi(\mathbf{r}) dl - \Theta(E) \int_{L_i} \theta(\mathbf{r}) dl\right) dE. \end{aligned} \quad (8)$$

Wu et al. [9] developed an optimal spectrum binning strategy, which uses a reduced number of energy bins instead of full spectrum information. Define  $(\phi_t, \theta_t)$  as the pairs of line integrals of photoelectric and Compton scatter components over total distance  $\mathbf{t}$  that are spaced over the equivalent range of materials,  $\mathbf{t} = [L_1 \ L_2 \ \dots \ L_M]$ . The approximated expected signals using spectrum binning can be expressed as

$$\hat{Y}^{\text{SB}}(\underline{\phi}_t, \underline{\theta}_t; \mathbf{B}_s, \Phi_s, \Theta_s) = \sum_{s=1}^S B_s \cdot \exp(-\Phi_s \phi_t - \Theta_s \theta_t) \quad (9)$$

$\Phi_s$  and  $\Theta_s$  are the corresponding values of each bin  $s$ . The energy bin sizes  $B_s$  need to satisfy the constraints that the sum of all bins is identical to the integral over the spectrum:

$$\sum_{s=1}^S B_s = \int_0^{E_{max}} b(E) dE, \quad B_s > 0 \quad \text{for } s = 1, 2, 3, \dots, S. \quad (10)$$

The optimal bin sizes  $\mathbf{B}_s$ , and the values of  $\Phi_s$  and  $\Theta_s$  are determined by optimizing

$$\arg \min_{\mathbf{B}_s, \Phi_s, \Theta_s} \|\log(\hat{Y}^{\text{full}}(\underline{\phi}_t, \underline{\theta}_t)) - \log(\hat{Y}^{\text{SB}}(\underline{\phi}_t, \underline{\theta}_t, \mathbf{B}_s, \Phi_s, \Theta_s))\|_1. \quad (11)$$

Empirical results show that the  $L_1$  distance provides relatively good BHC results.

## C. MMBHC-SB

Define  $\hat{p}_i(E) = \int_{L_i} \mu(E, \mathbf{r}) dl$  as the line integral through the volume along ray  $i$ . From Eq. (2) and (3),  $\hat{p}_i(E)$  can be written as

$$\hat{p}_i(E) = \sum_{m=1}^M \int_{L_i} \kappa_m(E) \cdot \frac{f_m(\mathbf{r}) \cdot g_{initial}(\mathbf{r})}{\kappa_m(E_0)} dl. \quad (12)$$

From the MMBHC approach, the spatial density image calculated from the original reconstruction is used instead of the true material density. A ratio density map is calculated as

$$\alpha_m(\mathbf{r}) = \frac{f_m(\mathbf{r}) \cdot g_{initial}(\mathbf{r})}{\rho_m \cdot \kappa_m(E_0)}. \quad (13)$$

The effective energy  $E_0$  should be material dependent. At the segmentation step, the updated centroids from k-means

clustering correspond to the effective attenuation coefficients for each material [11]. The effective energy of each material are then be determined.

Applying Eq. (7) and Eq. (13) to Eq. (12), the line integral  $\hat{p}^S$  for each discrete energy bin can be formulated as

$$\hat{p}_i^S = \Phi_s \sum_{m=1}^M \int_{L_i} \phi_m \alpha_m(\mathbf{r}) dl + \Theta_s \sum_{m=1}^M \int_{L_i} \theta_m \alpha_m(\mathbf{r}) dl. \quad (14)$$

The polychromatically reprojected sinogram can be calculated as

$$\hat{Y}_{\text{calc}}^{\text{MMBHC-SB}} = \sum_{s=1}^S B_s \cdot \exp(-\hat{p}_i^S). \quad (15)$$

#### D. Experiments

In order to evaluate the performance of the algorithm, polychromatic cone-beam CT simulations with added Poisson noise were carried out. The digital phantom has a soft tissue basis of 20 cm in diameter, two cortical bone columns of 4 cm in diameter and two titanium columns of 3 cm in diameter. Source-isocenter-distance is 80 cm and source-detector-distance is 120 cm. Each dataset consists of 640 projection images over an angular range of  $360^\circ$ , with a size of  $512 \times 512$  pixels at an isotropic resolution of  $0.8 \times 0.8 \text{ mm}^2$ . The image reconstruction was performed on a  $320 \times 320 \times 320$  voxel grid with spacing of  $0.8 \times 0.8 \times 0.8 \text{ mm}^3$ . Fig. 1 shows the attenuation coefficients of the three simulated materials and attenuation decomposition results for the case of cortical bone.

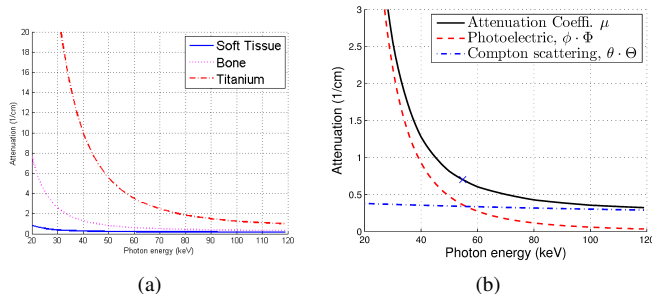


Fig. 1. (a) Attenuation coefficients of soft tissue, cortical bone and titanium. (b) Decomposition of attenuation coefficient into photoelectric and Compton scatter components for cortical bone (Eq. (6)).

### III. RESULTS AND DISCUSSION

The original reconstruction and correction results including line profiles are shown in Fig. 2. It can be seen that the FDK reconstruction suffers from cupping and streaking artifacts. The center image is obtained using the previous approach [8] with full spectrum information (120 energy bins), while the right image is calculated with a parameterized spectrum of three energy bins. Both are the correction results after the first iteration. The second row of Fig. 2 shows line profiles corresponding to each reconstructed image. It can be observed that the correction using three energy bins has comparable overall performance, with little over-correction on cortical bone. The material total lengths which are chosen for spectrum parameter optimization will result in different correction performance for each material.

As discussed before, since the polychromatic energy spectrum has different impact on different materials, the effective energy for each material has to be chosen independently. Table I shows effective energies of the three materials at each iteration. The values are obtained from k-means clustering of the reconstructed image, therefore segmentation errors which are caused by artifacts will influence the results. The segmentation improvement is illustrated in Fig. 3(a). The percentage of missegmented voxels converges quickly at the first iteration, further iterations only marginally improve the results. Fig. 3(b) shows the error volume of attenuations  $\log(\hat{Y}^{\text{full}}) - \log(\hat{Y}^S)$  corresponding to different materials' thicknesses. Maximum thickness values of different materials have been chosen according to relations between material attenuation coefficients at efficient energies.

Iterations	Soft tissue (keV)	Bone (keV)	Titanium (keV)
Original Recon.	58	72	91
1st iteration	65	71	85
2nd iteration	70	77	84
3rd iteration	71	76	84

TABLE I  
EFFECTIVE ENERGY FROM K-MEANS CLUSTERING FOR EACH MATERIAL AT EACH ITERATION.

Regarding computation time, the proposed algorithm has a large reduction of execution time for two reasons. Firstly, the number of polychromatic forward projection increases with the number of substances in the previous MMBHC approach. In the current method, increasing the material number only results in a marginal increase in computational time, because it forward projects the two components from attenuation decomposition. Moreover, the proposed approach only uses three energy bins in the polychromatic model instead of a full spectrum, which results in a significant reduction of computation load.

### IV. CONCLUSION

In this paper, we have derived an accelerated multi-material beam hardening correction approach using only a few energy bins instead of full spectrum information. As shown in the results, using the optimized three energy bins can provide effective beam hardening artifact reduction after the first iteration. The main advantage of the algorithm is the significant reduction of computation time. The number of forward and back-projections is not influenced by the number of materials, but depends on photoelectric and Compton scattering components obtained from attenuation decomposition.

#### ACKNOWLEDGMENT

The authors gratefully acknowledge funding of the Erlangen Graduate School in Advanced Optical Technologies (SAOT) by the German Research Foundation (DFG) in the framework of the excellence initiative.

**Disclaimer:** The concepts and information presented in this paper are based on research and are not commercially available.

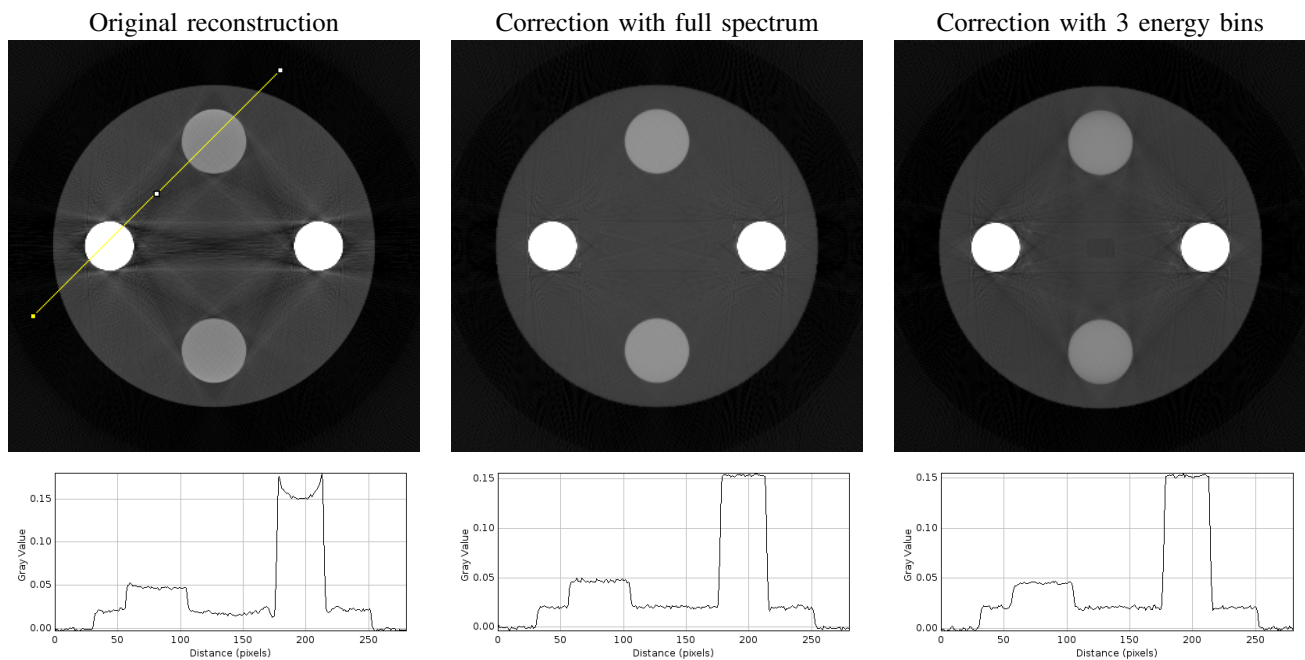


Fig. 2. Results of original analytical reconstruction, correction from previous MMBHC approach, and proposed algorithm with three energy bins. Corresponding line profiles are plotted. Correction images are results after the first iteration. Reconstructed images are displayed with window level  $[0.05; 0.09] \text{ mm}^{-1}$ .

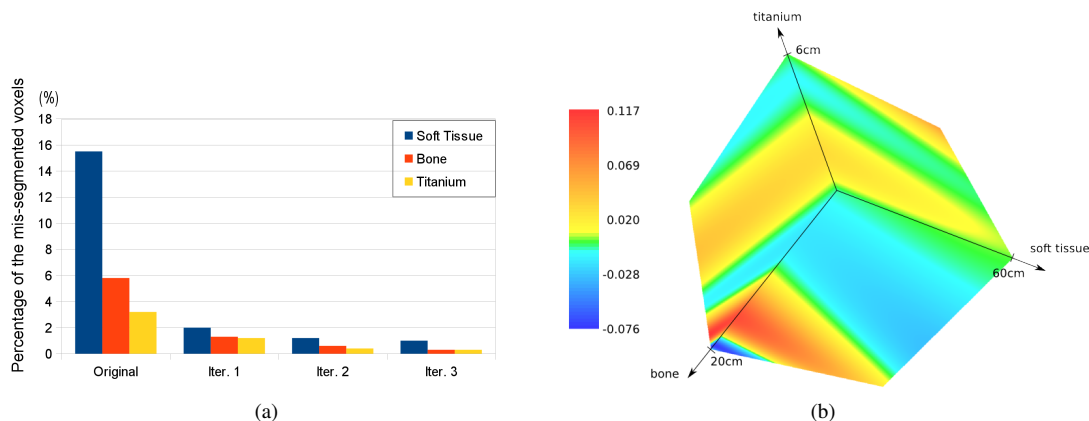


Fig. 3. (a) Percentage of incorrectly segmented voxels for three materials from original reconstruction and at each iteration step. (b) Attenuation error volume at three materials' various thicknesses using spectrum binning methods.

## REFERENCES

- [1] P. Joseph and R. Spital, "A method for correction bone induced artifacts in computed tomography scanners," *Journal of computer assisted tomography*, 1978.
- [2] M. Kachelriess, K. Sourbelle, and W. A. Kalender, "Empirical cupping correction: a first-order raw data pre-correction for cone-beam computed tomography," *Med Phys*, vol. 33, no. 5, pp. 1269–1274, May 2006.
- [3] C. Maaß, E. Meyer, and M. Kachelriess, "Exact dual energy material decomposition from inconsistent rays (MDIR)," *Medical Physics*, vol. 38, no. 2, pp. 691–700, 2011.
- [4] I. A. Elbakri and J. A. Fessler, "Statistical image reconstruction for polyenergetic X-ray computed tomography," *IEEE Trans Med Imaging*, vol. 21, no. 2, pp. 89–99, Feb. 2002.
- [5] B. De Man, J. Nuyts, P. Dupont, G. Marchal, and P. Suetens, "An iterative maximum-likelihood polychromatic algorithm for CT," *IEEE transactions on medical imaging*, vol. 20, no. 10, pp. 999–1008, Oct. 2001.
- [6] N. Menvielle, Y. Goussard, D. Orban, and G. Soulez, "Reduction of Beam-Hardening Artifacts in X-Ray CT," *Conference proceedings : Annual International Conference of the IEEE Engineering in Medicine and Biology Society*, vol. 2, pp. 1865–8, Jan. 2005.
- [7] G. Van Gompel, K. Van Slambrouck, M. Defrise, K. J. Batenburg, J. de Mey, J. Sijbers, and J. Nuyts, "Iterative correction of beam hardening artifacts in CT," *Medical physics*, vol. 38, no. 7, p. S36, Jul. 2011.
- [8] Q. Yang, N. Maass, M. Tian, M. Elter, I. Schasiepen, A. Maier, and J. Hornegger, "Multi-material beam hardening correction (MMBHC) in computed tomography," in *Proc. Intl. Mtg. on Fully 3D Image Recon. in Rad. and Nuc. Med*, 2013, pp. 533–536.
- [9] M. Wu, Q. Yang, A. Maier, and R. Fahrigr, "A practical statistical polychromatic image reconstruction for computed tomography using spectrum binning," in *SPIE 2014, to appear*, 02 2014.
- [10] Q. Yang, M. Wu, A. Maier, J. Hornegger, and R. Fahrigr, "Evaluation of spectrum mismatching using spectrum binning approach for statistical polychromatic reconstruction in CT," *Bildverarbeitung fuer die Medizin 2014, to appear*, 2014.
- [11] M. Tian, Q. Yang, A. Maier, I. Schasiepen, N. Maass, and M. Elter, "Automatic histogram-based initialization of k-means clustering in CT," in *Bildverarbeitung fuer die Medizin 2013*. Springer Berlin Heidelberg, 2013, pp. 277–282.